CrossMark
click for updates

Thermal atomic layer etching of crystalline aluminum nitride using sequential, self-limiting hydrogen fluoride and $Sn(acac)_2$ reactions and enhancement by H_2 and Ar plasmas

Nicholas R. Johnson, Huaxing Sun, and Kashish Sharma
Department of Chemistry and Biochemistry, University of Colorado at Boulder, Colorado 80309

Steven M. George[a)]
Department of Chemistry and Biochemistry, University of Colorado at Boulder, Colorado 80309 and Department of Mechanical Engineering, University of Colorado at Boulder, Colorado 80309

(Received 28 May 2016; accepted 13 July 2016; published 4 August 2016)

Thermal atomic layer etching (ALE) of crystalline aluminum nitride (AlN) films was demonstrated using sequential, self-limiting reactions with hydrogen fluoride (HF) and tin(II) acetylacetonate [$Sn(acac)_2$] as the reactants. Film thicknesses were monitored versus number of ALE reaction cycles at 275 °C using *in situ* spectroscopic ellipsometry (SE). A low etch rate of ~0.07 Å/cycle was measured during etching of the first 40 Å of the film. This small etch rate corresponded with the AlO_xN_y layer on the AlN film. The etch rate then increased to ~0.36 Å/cycle for the pure AlN films. *In situ* SE experiments established the HF and $Sn(acac)_2$ exposures that were necessary for self-limiting surface reactions. In the proposed reaction mechanism for thermal AlN ALE, HF fluorinates the AlN film and produces an AlF_3 layer on the surface. The metal precursor, $Sn(acac)_2$, then accepts fluorine from the AlF_3 layer and transfers an acac ligand to the AlF_3 layer in a ligand-exchange reaction. The possible volatile etch products are SnF(acac) and either $Al(acac)_3$ or $AlF(acac)_2$. Adding a H_2 plasma exposure after each $Sn(acac)_2$ exposure dramatically increased the AlN etch rate from 0.36 to 1.96 Å/cycle. This enhanced etch rate is believed to result from the ability of the H_2 plasma to remove acac surface species that may limit the AlN etch rate. The active agent from the H_2 plasma is either hydrogen radicals or radiation. Adding an Ar plasma exposure after each $Sn(acac)_2$ exposure increased the AlN etch rate from 0.36 to 0.66 Å/cycle. This enhanced etch rate is attributed to either ions or radiation from the Ar plasma that may also lead to the desorption of acac surface species. © *2016 American Vacuum Society.*
[http://dx.doi.org/10.1116/1.4959779]

I. INTRODUCTION

Atomic layer etching (ALE) is a sequential, self-limiting thin film removal technique that can etch materials precisely with Ångstrom-level precision. ALE is needed for future semiconductor manufacturing processes.[1] Until recently, most ALE processes have been conducted using halogen or halocarbon adsorption followed by energetic ion or atom bombardment to remove material.[2,3] This approach has been demonstrated for a variety of materials including Si,[4] Ge,[5] GaAs,[6] SiO_2,[7] HfO_2,[8] and graphene.[9] Etching with energetic ion or atom bombardment produces anisotropic material removal, but can also damage the underlying substrate.[8]

Recently, new ALE methods have been developed based on sequential, self-limiting thermal reactions.[10] Thermal ALE has been demonstrated for Al_2O_3 ALE and HfO_2 ALE using hydrogen fluoride (HF) and tin(II) acetylacetonate [$Sn(acac)_2$] as the reactants.[11–13] Al_2O_3 ALE has also been performed using HF and trimethylaluminum (TMA) as the reactants.[14] During the thermal ALE reactions, HF fluorinates the metal oxide and forms a metal fluoride layer on the surface.[10] The metal precursors, $Sn(acac)_2$ and TMA, then accept fluorine from the metal fluoride and transfer their ligands to the metal fluoride in a ligand-exchange reaction.[10] This transmetalation[15] or redistribution[16] process can form volatile species such as $AlF(acac)_2$ or $Al(acac)_3$.

The fluorination and ligand-exchange reactions have etched amorphous metal oxides such as Al_2O_3 and HfO_2 films that were grown using atomic layer deposition (ALD).[11–13] A related study also described the thermal ALE of amorphous AlF_3 films.[17] In contrast, there have been no reports for the thermal ALE of crystalline material. There have also been no previous demonstrations of the thermal ALE of a metal nitride, such as aluminum nitride (AlN), or any III–V semiconductor. However, the continuous dry etching of crystalline III–V metal nitrides, such as AlN, has been previously documented using different halogen plasma sources.[18–20] To extend the development of atomic layer processing methods, this letter presents the thermal ALE of crystalline AlN films using sequential, self-limiting exposures of HF and $Sn(acac)_2$ and the enhancement of the etching rates using plasma exposures. AlN ALE should be useful for the processing of AlN in high power and high temperature transistors, MEMS acoustic resonators, and photonic devices.[18–20]

II. EXPERIMENT

AlN samples were grown epitaxially on Si(111) wafers by Kyma Technologies using their plasma vapor deposition

[a)]Electronic mail: Steven.George@Colorado.Edu

Redistribution subject to AVS license or copyright; see http://scitation.aip.org/termsconditions. IP: 198.11.31.223 On: Thu, 04 Aug 2016 15:26:04

of nanocolumns (PVDNC^{TM}) crystal growth process. The AlN films are in the wurtzite crystalline phase with the (0001) plane parallel to the surface. The initial AlN films had a thickness of ∼500 Å. Etching of the AlN films was analyzed using *in situ* spectroscopic ellipsometry (SE) in a reaction chamber that has been described elsewhere.[21,22] This reaction chamber is very similar to plasma ALD reactors equipped for *in situ* ellipsometry measurements.[23] The chamber was pumped by a rotary vane pump (Alcatel 2010). The chamber was also equipped with a capacitance manometer for pressure measurements and a differentially pumped mass spectrometer for gas analysis. The base pressure of the reaction chamber was ∼10 mTorr.

The AlN films on the Si(111) wafers had dimensions of 1.5 × 1.5 cm. These samples were placed on a heated sample stage inside the reaction chamber. The temperature of the samples was held constant at 275 °C for all of the experiments. The walls of the chamber were held at ∼170 °C. $Sn(acac)_2$ (99.9%, Sigma-Aldrich) and HF-pyridine (70 wt. % HF, Sigma-Aldrich) were used as the reactants.[11–13] Each reactant was separately dosed into the chamber and held statically for 10 s. After each reactant exposure, the reaction chamber was purged with 80 sccm of ultrahigh purity (UHP) N_2 gas at a pressure of 840 mTorr for 130 s.

The AlN films were analyzed with *in situ* SE to obtain the film thickness after each reaction cycle or after each individual fluorination and ligand-exchange reaction. The AlN samples were analyzed with a Sellmeier model using the COMPLETE EASE software (J. A. Woollam). Because of the large bandgap of AlN at ∼6.2 eV, AlN behaves as a dielectric. AlN is not absorptive over the 0.73–5.18 eV spectral range of the SE analysis. Accurate thickness measurements can be obtained without a complex model accounting for light absorption. The fit of the Sellmeier model to the ψ and Δ ellipsometry parameters after removal of the AlO_xN_y layer yielded refractive indices in the range of 2.13–2.17. These refractive indices are in agreement with previous measurements for crystalline AlN.[24]

X-ray photoemission spectroscopy (XPS) analysis was performed using a PHI 5600 x-ray photoelectron spectrometer using a monochromatic Al Kα source. The XPS depth-profiling was obtained using Ar ion sputtering. The XPS data were collected using AugerScan (RBD Instruments) and analyzed in CASAXPS (Casa Software, Ltd.). The x-ray reflectivity (XRR) scans were recorded by a high resolution x-ray diffractometer (Bede D1, Jordan Valley Semiconductors) using Cu Kα ($\lambda = 1.540$ Å) radiation. The analysis software (Bede REFS, Jordan Valley Semiconductors) fitted the XRR scans to determine film thicknesses.

The reactor was equipped with a remote inductively coupled plasma (ICP) source. The ICP plasma source was positioned with the opening roughly 3–4 cm above the heated sample stage. The ICP source was a quartz tube (6 cm inner diameter × 25 cm long) surrounded by a copper helical coil. The ICP was generated using a 13.56 MHz RF generator (Paramount RF Power Supply, Advanced Energy) and 50 Ω impedance matching network (Navigator Digital Matching Network, Advanced Energy).

III. RESULTS AND DISCUSSION

Figure 1 shows the etching of a typical AlN sample for 600 reaction cycles at 275 °C under self-limiting reaction conditions with an HF exposure of 1270 mTorr s and a $Sn(acac)_2$ exposure of 900 mTorr s. The slow etch rate over the first 300 reaction cycles is attributed to an AlO_xN_y layer on the surface of the AlN film. The etch rate in this AlO_xN_y region is ∼0.07 Å/cycle. After a thickness change of ∼30 Å corresponding with ∼300 ALE reaction cycles, there is an increase in the etch rate. This increase is attributed to reaching a purer AlN film with less oxidation. After a thickness change of ∼50 Å corresponding with ∼400 ALE reaction cycles, the etch rate increases to ∼0.36 Å/cycle in the pure AlN region.

To confirm the presence of an AlO_xN_y layer on the AlN film, the film composition was evaluated using x-ray photoelectron spectroscopy (XPS). Figure 2 displays the results of an XPS depth-profile experiment versus sputtering time. Figure 2 indicates that there is a large concentration of oxygen on the surface that decays as a function of sputtering time. The oxygen concentration in the bulk of the AlN film is only ∼1.5–2.0 at. %. Using the sputtering time and the Si XPS signal as a marker for the removal of the entire AlN film with an initial thickness of ∼500 Å, the thickness of the AlO_xN_y layer is estimated to be ∼40 Å. This AlO_xN_y layer thickness agrees with the etching results in Fig. 1. The thickness of the AlO_xN_y layer is also consistent with x-ray reflectivity (XRR) experiments that yield an oxide thickness of ∼44 Å on the AlN film. The AlO_xN_y layer thickness is slightly higher than the typical oxide thicknesses of ∼20–30 Å reported on AlN samples exposed to ambient air at room temperature.[25,26] Figure 2 also observes that the AlN films are Al-rich in agreement with previous XPS characterization by Kyma Technologies. Similar Al-rich AlN films are

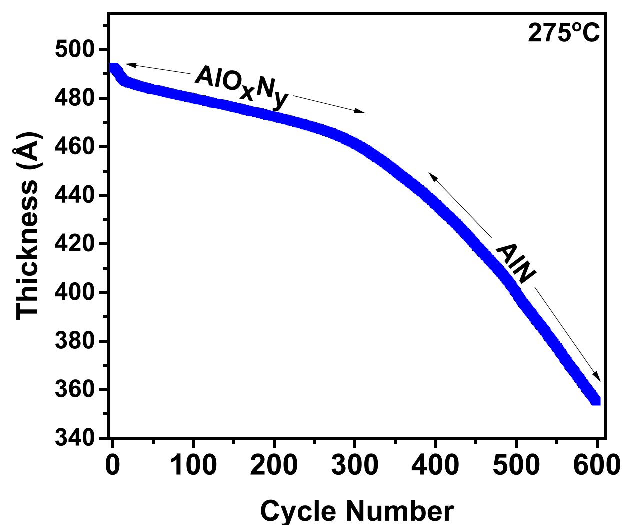

FIG. 1. (Color online) Film thickness measured by spectroscopic ellipsometry vs number of AlN ALE reaction cycles at 275 °C. The etch rate increases after removing the AlO_xN_y layer on the AlN film.

Redistribution subject to AVS license or copyright; see http://scitation.aip.org/termsconditions. IP: 198.11.31.223 On: Thu, 04 Aug 2016 15:26:04

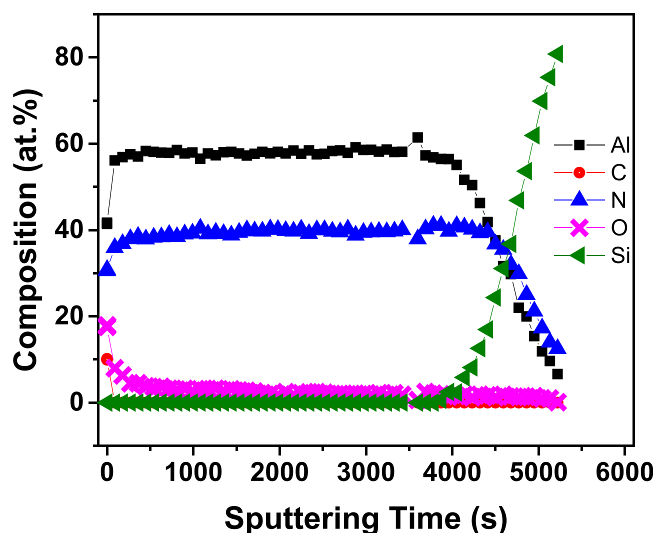

FIG. 2. (Color online) Film composition vs sputter time obtained by XPS depth-profiling analysis. The initial AlN film on the Si(111) wafer had a thickness of ~500 Å.

reported by XPS depth-profiling studies of AlN films grown using various techniques.[27–29]

Figure 3 investigates the self-limiting nature of the HF and $Sn(acac)_2$ reactions during the AlN ALE reactions at 275 °C. Etch rates were determined by varying one reactant exposure while keeping the other reactant exposure constant. Figure 3(a) depicts the self-limiting behavior of the HF reaction with a $Sn(acac)_2$ exposure of 900 mTorr s defined by a $Sn(acac)_2$ exposure time of 10 s and a $Sn(acac)_2$ pressure of 90 mTorr. The HF exposures were changed from 254 to 1730 mTorr s using an HF exposure time of 10 s and different HF pressures. The reaction chamber was purged with 80 sccm of UHP N_2 gas at a pressure of 840 mTorr for 130 s after each reactant exposure.

Figure 3(a) shows that small etch rates were observed for low HF exposures when the surface has not yet formed a saturated fluoride layer thickness. After an exposure of 966 mTorr s, the fluorination by HF has reached self-limiting conditions and the etch rate is ~0.36 Å/cycle. The slight increase in the etch rate at an HF exposure of 1730 mTorr s is likely caused by chemical vapor etching. HF has a long residence time in the reaction chamber and purge times over 10 min are needed to remove HF from the reactor after large HF exposures.

Figure 3(b) demonstrates the self-limiting nature of the $Sn(acac)_2$ reaction. $Sn(acac)_2$ exposures were varied while HF exposures were held constant at an exposure of 1270 mTorr s defined by a HF exposure time of 10 s and a HF pressure that varied between 140 and 110 mTorr. The $Sn(acac)_2$ exposures were varied from 300 to 1200 mTorr s using an exposure time of 10 s and different $Sn(acac)_2$ pressures. The etch rate slowly increases with $Sn(acac)_2$ exposure until reaching an etch rate of ~0.36 Å/cycle at an $Sn(acac)_2$ exposure of 900 mTorr s. At this point, the $Sn(acac)_2$ reaction is self-limiting. Both Figs. 3(a) and 3(b) show self-limiting behavior with an AlN etch rate of ~0.36 Å/cycle.

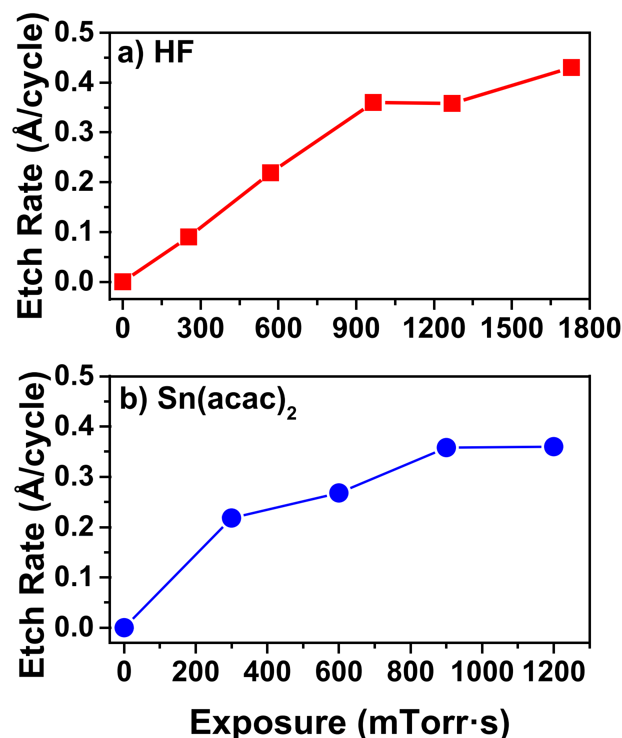

FIG. 3. (Color online) Etch rate vs reactant exposure during AlN ALE at 275 °C. (a) Etch rate vs HF exposure with $Sn(acac)_2$ exposure fixed at 900 mTorr s and (b) etch rate vs $Sn(acac)_2$ exposure with HF exposure fixed at 1270 mTorr s.

Figure 4 shows an expansion of a section of Fig. 1 for 21 AlN ALE reaction cycles corresponding to reaction cycles No. 471–491 under self-limiting reaction conditions. The change in AlN thickness versus number of ALE reaction cycles is linear. The measured etch rate of 0.38 Å/cycle is consistent with the etch rate of ~0.36 Å/cycle determined by the self-limiting studies displayed in Fig. 3. Numerous experiments were performed for AlN ALE at 275 °C. The measured etch rates varied from 0.34 to 0.38 Å/cycle and the majority of the individual measurements yielded an etch rate of 0.36 Å/cycle.

The proposed reaction mechanism for thermal AlN ALE is similar to the reaction mechanism proposed for Al_2O_3 ALE and HfO_2 ALE.[11–13] During the HF exposure, the HF fluorinates the AlN film and produces an AlF_3 layer on the surface and NH_3 as a volatile reaction product. AlF_3 is a very stable metal fluoride with a sublimation point at 1291 °C. The metal precursor, $Sn(acac)_2$, then accepts fluorine from the AlF_3 layer and transfers an acac ligand to the AlF_3 layer in a ligand-exchange reaction. This ligand-exchange process is believed to occur via a four-center transition state.[10,15] For AlN ALE using HF and $Sn(acac)_2$, this four-center transition state would be defined by F and acac ligands bridging between the Sn and Al metal centers. The probable reaction products of the ligand-exchange process are SnF(acac) and either $AlF(acac)_2$ or $Al(acac)_3$ as volatile etch products. A similar reaction mechanism based on a combination of AlN ALE and Al_2O_3 ALE would also apply for the etching of the AlO_xN_y layer.[11,12]

Redistribution subject to AVS license or copyright; see http://scitation.aip.org/termsconditions. IP: 198.11.31.223 On: Thu, 04 Aug 2016 15:26:04

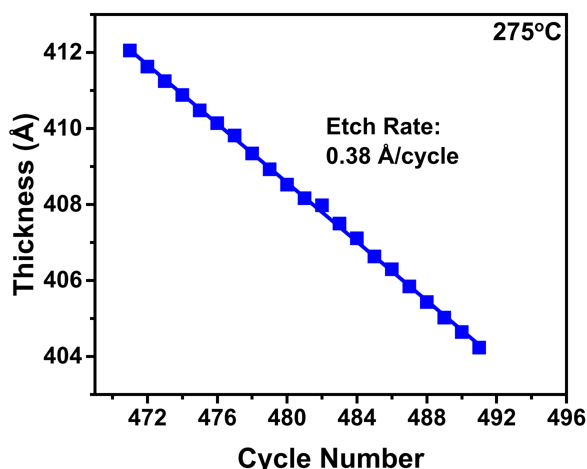

FIG. 4. (Color online) Film thickness vs number of AlN ALE reaction cycles at 275 °C in pure AlN region of AlN film. Change of thickness vs number of AlN ALE reaction cycles gives an etch rate of 0.38 Å/cycle.

The effect of H_2 plasma exposure on thermal AlN ALE was also examined using *in situ* SE analysis. Plasma exposures are known to enhance ALD and similar plasma effects may be beneficial during thermal ALE.[30] During the H_2 plasma experiments, the reactant exposures and purge times were the same as the reactant exposures and purge times used for thermal ALE. The H_2 plasma exposure was added after each Sn(acac)$_2$ exposure. The H_2 plasma with a power of 100 W was generated at a H_2 pressure of 40 mTorr and exposed to the surface for 15 s. After the H_2 plasma exposure, the chamber was purged for 60 s with the same conditions as used for the HF and Sn(acac)$_2$ reactants.

Figure 5(a) shows the effect of adding the H_2 plasma exposure after the Sn(acac)$_2$ exposure during each thermal ALE reaction cycle. These thickness measurements were performed in the pure AlN region of the AlN film. The etch rate increases from 0.36 Å/cycle for thermal ALE to 1.96 Å/cycle for H_2 plasma-enhanced thermal ALE. This large increase in the etch rate is attributed to the removal of acac surface species by H radicals from the H_2 plasma. Earlier experiments have shown that acac surface species may block surface sites and limit the etching during thermal Al_2O_3 ALE with HF and Sn(acac)$_2$ as the reactants.[12] Removal of these blocking species may allow for more HF to fluorinate the surface and, subsequently, for more ligand-exchange with Sn(acac)$_2$. Additionally, heat released by recombination of H radicals may facilitate desorption of the acac surface species.[31] The H_2 plasma by itself did not etch the AlN film unless the H_2 plasma was used in conjunction with the thermal ALE reaction cycles.

Similar experiments were performed using an argon plasma exposure instead of the H_2 plasma exposure. The Ar plasma with a power of 100 W was generated at an Ar pressure of 40 mTorr and exposed to the surface for 15 s. Figure 5(b) displays the effect of adding the Ar plasma exposure after the Sn(acac)$_2$ exposure during each thermal ALE reaction cycle. After the Ar plasma exposure, the chamber was purged for 60 s with the same conditions as used for the HF and Sn(acac)$_2$ reactants. In this case, the etch rate for AlN

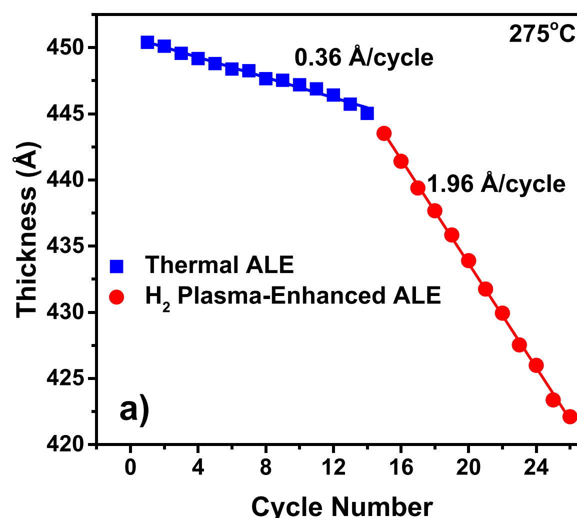

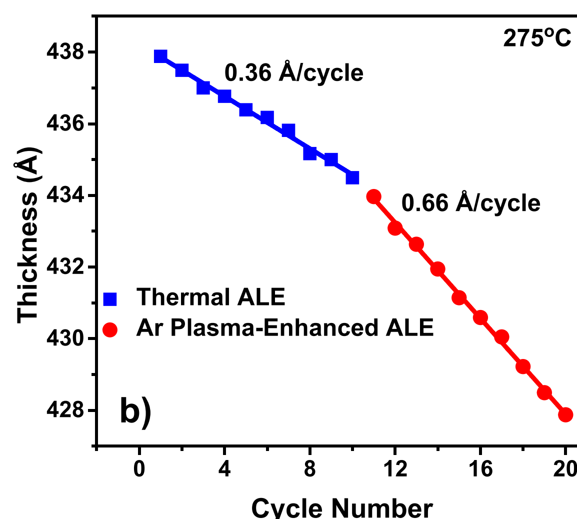

FIG. 5. (Color online) Film thickness vs number of AlN ALE reaction cycles at 275 °C in pure AlN region of AlN film showing results for thermal AlN ALE and plasma-enhanced ALE. (a) H_2 plasma increases AlN etch rate from 0.36 to 1.96 Å/cycle. (b) Ar plasma increases AlN etch rate from 0.36 to 0.66 Å/cycle.

ALE increases from 0.36 Å/cycle for thermal ALE to 0.66 Å/cycle for the plasma-enhanced thermal ALE. Because the Ar plasma is not a source of reactive radicals, the increase in the etch rate for AlN ALE from the Ar plasma indicates that ions or radiation produced by the Ar plasma may be enhancing the AlN ALE. The Ar plasma did not change the AlN film thickness unless the Ar plasma was employed together with the thermal ALE reaction cycles.

Recent studies have explored the effect of plasmas on ALD processing.[30,32] Plasmas are believed to enhance ALD reactions primarily through reactive radical species. However, ions and radiation produced by plasmas can also influence surface reactions.[32] The enhancement of the etch rate for AlN ALE by the Ar plasma indicates that ions or radiation may be playing a role. The ions from ICP sources typically have energies <50 eV and could desorb the acac surface species that may limit the etching.[30,32] Ar plasmas also have a variety of optical emission lines at wavelengths <200 nm that have photon energies larger than the AlN

Redistribution subject to AVS license or copyright; see http://scitation.aip.org/termsconditions. IP: 198.11.31.223 On: Thu, 04 Aug 2016 15:26:04

bandgap at ∼6.2 eV.[33] These photons may be able to photodesorb acac surface species or excite electron/hole pairs by bandgap excitation that may lead to desorption. Optical emission from the H_2 plasma may also be adding to the effect of H radicals on thermal AlN ALE.[30]

The plasma enhancement effects on thermal ALE are very promising. Thermal ALE will be valuable for etching three-dimensional nanostructures, such as semiconductor nanowires, because thermal ALE is expected to be isotropic and conformal.[1] The plasma enhancement effects on thermal ALE from ions can facilitate anisotropic etching that will be useful for fabricating high aspect ratio nanodevices.[10] In addition, the plasma enhancement of thermal ALE will also lower the required processing temperatures for semiconductor nanofabrication.

IV. CONCLUSIONS

The thermal ALE of crystalline AlN was performed using sequential, self-limiting HF and $Sn(acac)_2$ reactions. This is the first demonstration of the thermal ALE of a metal nitride and the first report of the thermal ALE of a crystalline III–V material. At self-limiting reaction conditions, the etch rate for AlN ALE was 0.36 Å/cycle at 275 °C. These results suggest that other similar crystalline III–V metal nitrides, such as GaN and InN, should also be etched using HF and $Sn(acac)_2$. H_2 or Ar plasma exposures increased the AlN etch rate to 1.96 or 0.66 Å/cycle, respectively, at 275 °C. The plasma enhancement of thermal ALE should be useful for introducing anisotropic etching and also for lowering the temperatures required for etching. Thermal ALE and plasma-enhanced thermal ALE have great promise for etching a number of important materials and expanding the tool set for advanced semiconductor manufacturing.

ACKNOWLEDGMENTS

This work was supported by the Defense Advanced Research Projects Agency (DARPA) under Grant No. W911NF-13-1-0041. The authors thank Tyler McQuade from DARPA for his support and encouragement. The authors also acknowledge Advanced Energy in Fort Collins, Colorado, for the RF power supply and impedance matching network for the ICP plasma source.

[1] C. T. Carver, J. J. Plombon, P. E. Romero, S. Suri, T. A. Tronic, and R. B. Turkot, ECS J. Solid State Sci. Technol. **4**, N5005 (2015).
[2] V. M. Donnelly and A. Kornblit, J. Vac. Sci. Technol., A **31**, 050825 (2013).
[3] K. J. Kanarik, T. Lill, E. A. Hudson, S. Sriraman, S. Tan, J. Marks, V. Vahedi, and R. A. Gottscho, J. Vac. Sci. Technol., A **33**, 020802 (2015).
[4] S. D. Athavale and D. J. Economou, J. Vac. Sci. Technol., B **14**, 3702 (1996).
[5] T. Sugiyama, T. Matsuura, and J. Murota, Appl. Surf. Sci. **112**, 187 (1997).
[6] W. S. Lim, S. D. Park, B. J. Park, and G. Y. Yeom, Surf. Coat. Technol. **202**, 5701 (2008).
[7] D. Metzler, R. L. Bruce, S. Engelmann, E. A. Joseph, and G. S. Oehrlein, J. Vac. Sci. Technol., A **32**, 020603 (2014).
[8] J. B. Park, W. S. Lim, B. J. Park, I. H. Park, Y. W. Kim, and G. Y. Yeom, J. Phys. D: Appl. Phys. **42**, 055202 (2009).
[9] W. S. Lim *et al.*, Carbon **50**, 429 (2012).
[10] S. M. George and Y. Lee, ACS Nano **10**, 4889 (2016).
[11] Y. Lee and S. M. George, ACS Nano **9**, 2061 (2015).
[12] Y. Lee, J. W. DuMont, and S. M. George, Chem. Mater. **27**, 3648 (2015).
[13] Y. Lee, J. W. DuMont, and S. M. George, ESC J. Solid State Sci. Technol. **4**, N5013 (2015).
[14] Y. Lee, J. W. DuMont, and S. M. George, Chem. Mater. **28**, 2994 (2016).
[15] K. Osakada, "Tranmetalation," in *Fundamentals of Molecular Catalysis, Current Methods in Inorganic Chemistry*, edited by H. Kurosawa and A. Yamamoto (Elsevier Science, Amsterdam, 2003), Vol. 3.
[16] J. C. Lockhart, Chem. Rev. **65**, 131 (1965).
[17] Y. Lee, J. W. DuMont, and S. M. George, J. Phys. Chem. C **119**, 25385 (2015).
[18] D. Chen, D. Xu, J. Wang, B. Zhao, and Y. Zhang, Vacuum **83**, 282 (2008).
[19] S. J. Pearton, C. R. Abernathy, and F. Ren, Appl. Phys. Lett. **64**, 2294 (1994).
[20] R. J. Shul, C. G. Willison, M. M. Bridges, J. Han, J. W. Lee, S. J. Pearton, C. R. Abernathy, J. D. MacKenzie, and S. M. Donovan, Solid-State Electron. **42**, 2269 (1998).
[21] J. W. Clancey, A. S. Cavanagh, R. S. Kukreja, A. Kongkanand, and S. M. George, J. Vac. Sci. Technol., A **33**, 01A130 (2015).
[22] A. S. Cavanagh, L. Baker, J. W. Clancey, J. Yin, A. Kongkanand, F. T. Wagner, and S. M. George, ECS Trans. **58**, 19 (2013).
[23] E. Langereis, S. B. S. Heil, H. C. M. Knoops, W. Keuning, M. C. M. van de Sanden, and W. M. M. Kessels, J. Phys. D: Appl. Phys. **42**, 073001 (2009).
[24] H. Y. Joo, H. J. Kim, S. J. Kim, and S. Y. Kim, J. Vac. Sci. Technol., A **17**, 862 (1999).
[25] M. Sternitzke, J. Am. Ceram. Soc. **76**, 2289 (1993).
[26] J. H. Edgar, L. Du, L. Nyakiti, and J. Chaudhuri, J. Cryst. Growth **310**, 4002 (2008).
[27] N. Laidani, L. Vanzetti, M. Anderle, A. Basillais, C. Boulmer-Leborgue, and J. Perriere, Surf. Coat. Technol. **122**, 242 (1999).
[28] L. Rosenberger, R. Baird, E. McCullen, G. Auner, and G. Shreve, Surf. Interface Anal. **40**, 1254 (2008).
[29] Y. Watanabe, Y. Hara, T. Tokuda, N. Kitazawa, and Y. Nakamura, Surf. Eng. **16**, 211 (2000).
[30] H. B. Profijt, S. E. Potts, M. C. M. van de Sanden, and W. M. M. Kessels, J. Vac. Sci. Technol., A **29**, 050801 (2011).
[31] R. K. Grubbs and S. M. George, J. Vac. Sci. Technol., A **24**, 486 (2006).
[32] H. B. Profijt, P. Kudlacek, M. C. M. van de Sanden, and W. M. M. Kessels, J. Electrochem. Soc. **158**, G88 (2011).
[33] J. W. Carr and M. W. Blades, Spectrochim. Acta, Part B **39**, 567 (1984).

Redistribution subject to AVS license or copyright; see http://scitation.aip.org/termsconditions. IP: 198.11.31.223 On: Thu, 04 Aug 2016 15:26:04